The heavy atom structure, "cis effect" on methyl internal rotation, and 14 N nuclear quadrupole coupling of 1-cyanopropene from quantum chemical and microwave spectroscopic analysis

Truong Anh Nguyen, Isabelle Kleiner, Martin Schwell, Ha Vinh Lam Nguyen

FULL PAPER

The heavy atom structure, "*cis* effect" on methyl internal rotation, and ^{14}N nuclear quadrupole coupling of 1-cyanopropene from quantum chemical and microwave spectroscopic analysis

Truong Anh Nguyen,[a] Isabelle Kleiner,[a] Martin Schwell,[b] and Ha Vinh Lam Nguyen*[b][c]

Abstract: The microwave spectrum of 1-cyanopropene (crotonitrile) was remeasured using two pulsed molecular jet Fourier transform microwave spectrometers operating from 2.0 to 40.0 GHz. The molecule exists in two isomer forms, *E* and *Z*, with respect to the orientation between the methyl and the cyano groups. The spectrum of the *Z* isomer is more intense. Due to internal rotation of the methyl group, doublets containing A and E torsional species were found for all rotational transitions. Hyperfine splittings arising from the ^{14}N nuclear quadrupole coupling were resolved. The heavy atom structure of the *Z* isomer was determined by observation of ^{13}C and ^{15}N isotopologue spectra in natural abundances. The experimental results were supported by quantum chemistry. The complex spectral patterns were analyzed and fitted globally, and the barriers to methyl internal rotation are determined to be 478.325(28) cm^{-1} and 674.632(76) cm^{-1} for the *Z* and *E* isomers, respectively. The non-bonded intramolecular electrostatic attraction between the methyl group and the 1-cyano substituent overcomes steric hindrance, leading to higher stability of the *Z* isomer. The consequence is a slight opening of 3.2° of the C(1)-C(2)-C(3) angle and a radical decrease of the methyl torsional barrier in the Z isomer due to steric repulsion.

1. Introduction

Microwave spectroscopy is known in physical chemistry for its power in determining molecular structures in the gas phase with outstanding precision. In particular, it allows the experimental distinction between different conformers and isomers of the same molecule. The sensitivity and resolution of the pulsed jet Fourier transform technique enable even the distinction of minor isotopologues such as ^{13}C and ^{15}N in natural abundances of 1.11% and 0.37%,[1] respectively. Since changing a ^{12}C atom by a ^{13}C atom or a ^{14}N atom by a ^{15}N atom leads to a different total molecular mass, the mass distributions within the molecule change and consequently, the rotational signature also changes and serves as a unique identification of molecular species. The experimentally determined rotational constants can then be utilized to deduce atomic positions, bond lengths, and bond angles.[2]

[a] Université Paris Cité and Univ Paris Est Creteil, CNRS, LISA, F-75013 Paris, France
[b] Univ Paris Est Creteil and Université Paris Cité, CNRS, LISA, F-94010 Créteil, France
[c] Institut Universitaire de France (IUF), F-75231 Paris, France

* Corresponding author:
Ha Vinh Lam Nguyen
Univ Paris Est Creteil and Université Paris Cité, CNRS, LISA, F-94010 Créteil, France
Institut Universitaire de France (IUF), F-75231 Paris, France
E-mail: lam.nguyen@lisa.ipsl.fr

Supporting information for this article is given via a link at the end of the document.

Regarding its applications, microwave spectroscopy is an essential tool for interstellar chemistry, providing, as one of the main contributors, line lists for astrophysical investigations that allow the detection of new molecular species in space. For example, the discovery of methyl acetate and ethyl formate in the Orion molecular cloud was only possible after a considerable amount of previous microwave spectroscopic analyses of these molecules in the laboratory.[3] The number of molecular species detected in the interstellar medium (ISM) or in the circumstellar envelopes (CSE) of stars has increased to 200 during about 80 years, since the existence of molecules in the ISM has been proven in 1940,[4] and exploded to over 300 within the last few years. The complete list of discovered molecules is summarized in the Cologne Database for Molecular Spectroscopy (CDMS) website.[5] Even larger and heavier complex organic molecules, defined as carbon-bearing species with more than five atoms, have entered the list. However, despite the rapid tempo of detecting new molecular species, recorded telescope surveys are still overwhelmed by unidentified lines that cannot be assigned to any molecule using the currently available spectroscopic linelists.[6] An important number of these lines might arise from minor isotopologues of already detected species that lack spectroscopic characterizations.[7]

Fully or nearly saturated molecules are especially abundant in the hottest and densest parts of star-forming regions. It is remarkable that many molecules recently detected in space contain a cyanide bond, *i.e.*, the first molecule containing a benzene ring, benzonitrile, detected in 2018,[8] propargyl cyanide,[9] cyanocyclopentadiene,[10] vinylcyanoacetylene and cyanovinylacetylene,[11] cyanoacetyleneallene,[12] cyanonaphthalene,[13] cyanovinyl radical H_2CCCN,[14] and recently five cyano-derivatives of propene.[15] The detection of two isomers of 1-cyanopropene (crotonitrile), *cis* (hereinafter called the *Z* isomer) and *trans* (hereinafter called the *E* isomer), in the Taurus Molecular Cloud TCM-1 using the QUIJOTE survey covering the spectral range 31.0-50.4 GHz[15] was based on previous microwave and millimeterwave investigations, first by Beaudet[16] for the *Z* isomer, then by Suzuki and Kozima[17] as well as Hsu and Flygare[18] for the *E* isomer, and later by Lesarri et al.[19] for both. 1-cyanopropene experiences two quantum mechanical effects that influence the positions of microwave spectral lines: the internal rotation of the methyl group and the nuclear quadrupole coupling of the ^{14}N atom. The methyl internal rotation causes all rotational transitions in the spectrum to split into the so-called A-E doublets. The ^{14}N nuclear quadrupole coupling adds a hyperfine structure on each torsional species, making each rotational transition appear as multiplets with complicated spectral patterns and different intensities. No studies on the minor isotopologues of 1-cyanopropene exist in the literature.

We decided to revisit the microwave spectrum of this molecule in the frequency range from 2 to 40 GHz using two molecular jet Fourier Transform MicroWave (FTMW) spectrometers [20],[21] with several goals. Firstly, (i) the high sensitivity of the instruments enabled measurements of the spectra of the ^{13}C and ^{15}N minor isotopologues of *Z*-1-cyanopropene to determine for the first time their frequency lists and the heavy atom microwave structure. Secondly, (ii) in the study of Lesarri et al.,[19] the methyl internal rotation splittings of the *Z* isomer were fitted using Woods' IAM program [22] to deduce the torsional barrier, but the rotational constants and the centrifugal distortion constants were determined by fitting only A species transitions. Therefore, they are effective and have lost their physical meaning for molecular geometry and centrifugal distortion effect. We applied two internal rotation programs frequently used in the microwave spectroscopic community, *XIAM*[23] and *BELGI-Cs-hyperfine*[24] to fit the two effects globally. The global fitting was also carried out for all minor isotopologue fits, since physically meaningful rotational constants are important when they are used as input for structure determination. Furthermore, many of the weak *b*-type transitions have not been detected in Ref. [19], causing slightly higher errors on the determined rotational constants. With not only the high resolution but also the high sensitivity of the used FTMW spectrometers, it was possible to detect most of the *a*- and *b*-type transitions up to $J = 8$, improving thus the accuracy of the determined constants. (iii) We also aim at resolving the methyl internal rotation splittings of the *E* isomer to determine precisely its torsional barrier using the high resolution of the two molecular jet FTMW spectrometers. The A-E doublets were not resolved for the *E* isomer in Ref. [19], and the torsional barrier reported in Refs. [17] and [18] was not very precise. (iv) Finally, we performed a vast amount of quantum chemical calculations for benchmarking purpose. To assign rotational spectra, it is necessary to have a fairly reliable estimation of the rotational constants. The rapid development of modern quantum chemistry has made it possible to calculate equilibrium structures at affordable costs to access the rotational constants theoretically. However, it is not always clear which level of theory should be chosen for calculations for an optimal ratio between computational cost and reliability in predicting rotational constants. To find out an optimum level for propene derivatives, we calculated the rotational constants of both 1-cyanopropene isomers at different levels of theory to compare with the experimental ones.

2. Quantum Chemical Calculations

2.1. Geometry Optimizations

The target molecule 1-cyanopropene shown in Figure 1 consists of an unsaturated hydrocarbon chain with a C=C double bond and a C≡N triple bond. The configuration with the methyl group located at the same side with the cyano group is denoted as the *Z* isomer (*zusammen*), while for the *E* isomer (*entgegen*), the two groups are located at different sides of the double bond. The geometry optimizations were performed at different levels of theory using several method and basis set combinations using the *Gaussian 16* program package.[25]. Density functional theory methods in use are B3LYP-D3,[26-28] B3LYP-D3BJ,[29] CAM-B3LYP,[30] ωB97X-D,[31] Perdew-Burke-Ernzerhof (PBE0),[32] MN15,[33] and M06-2X[34]; *ab initio* methods are MP2[35] and CCSD.[36] These methods were combined with several basis sets, such as Dunning's polarized valence double- (cc-pVDZ) and triple-zeta (cc-pVTZ),[37] with or without diffuse functions included in the augmented basis sets (aug). Pople's basis sets[38] (6-31G or 6-311G) with or without diffuse functions (+ or ++) were also utilized with polarization functions like (d,p), (df,dp), (2d,2p), (2df,2pd), (3df,3dp) included in all cases. The optimized structures of both isomers are illustrated in Figure 1. The equilibrium rotational constants B_e^{ξ} (with ξ = *a*, *b*, *c*) and dipole moment components calculated at two chosen levels, MP2/6-311++G(d,p) and B3LYP-D3BJ/6-311++G(d,p), are presented in Table 1. The atomic coordinates from geometries optimized at these two levels are in Table S-1 in the Supplementary Materials. The complete lists of predicted rotational constants are collected in Table S-2. All atoms of the molecule except two hydrogen atoms of the methyl group are located on the same plane, *i.e.*, the C_s symmetry plane. The *Z* isomer is about 1.2 kJ/mol lower in energy than the *E* isomer and is thus the more stable configuration. Anharmonic frequency calculations were performed at the MP2/6-311++G(d,p) and

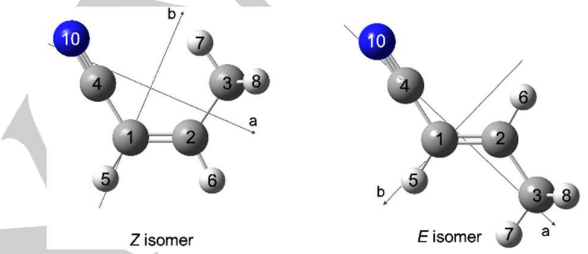

Figure 1. Geometries of the *Z* and the *E* isomers of 1-cyanopropene. The hydrogen H_9 is located behind H_8 in both isomers. Hydrogen atoms are marked in white, the carbon atoms are in dark grey and the nitrogen atom is in blue.

Table 1. Equilibrium rotational constants A_e, B_e, C_e, vibrational ground state rotational constants A_0, B_0, C_0, centrifugal distortion constants in the asymmetrically reduced Hamiltonian obtained from anharmonic frequency calculations, dipole moment components μ_a, μ_b, μ_c, V_3 potential energy of the methyl internal rotation, and relative energy ΔE_{ZPE} (with zero-point corrections) of the two isomers of 1-cyanopropene calculated at the MP2/6-311++G(d,p) and B3LYP-D3BJ/6-311++G(d,p) levels of theory.

		***Z* isomer**		***E* isomer**	
		MP2	B3LYP-D3BJ	MP2	B3LYP-D3BJ
A_e	MHz	11802.0	12102.4	37909.0	38723.4
B_e	MHz	3480.5	3469.9	2276.8	2296.9
C_e	MHz	2733.4	2742.2	2176.8	2197.6
A_0	MHz	11742.8	12046.9	37668.7	38515.8
B_0	MHz	3470.4	3458.7	2266.8	2286.9
C_0	MHz	2720.9	2729.3	2166.6	2187.5
Δ_J	kHz	2.6517	2.5128	0.2703	0.2684
Δ_{JK}	kHz	−18.0843	−17.9101	−16.9188	−16.4148
Δ_K	MHz	0.0653	0.0678	0.8780	0.8707
δ_J	kHz	0.8458	0.7908	0.0286	0.0276
δ_K	kHz	4.9990	4.9174	−0.1550	−0.2480
$\lvert\mu_a\rvert$	D	3.69	4.06	4.43	4.83
$\lvert\mu_b\rvert$	D	1.57	1.60	0.60	0.55
$\lvert\mu_c\rvert$	D	0.00	0.00	0.00	0.00
V_3	cm^{-1}	447.7	483.1	672.2	657.8
ΔE_{ZPE}	kJ/mol	0	0	1.18	1.30

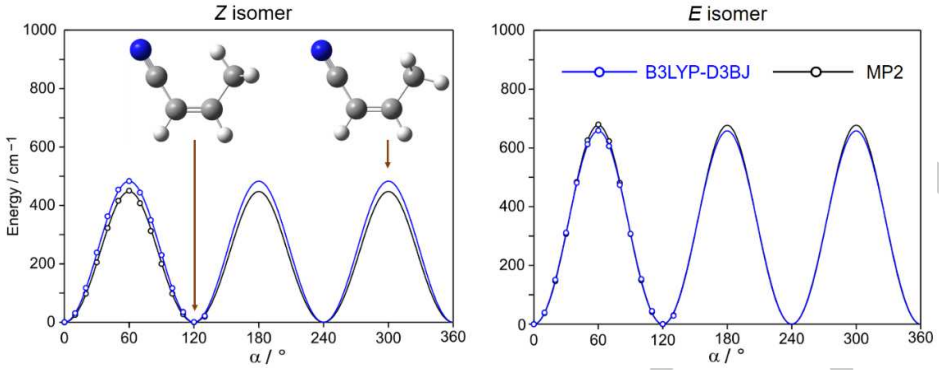

Figure 2. Potential energy curves for the *Z* isomer (left hand side) and the *E* isomer (right hand side) of 1-cyanopropene calculated by varying the dihedral angles $\alpha = \angle(C_2, C_3, C_4, H_7)$, corresponding to the internal rotation of the methyl group. For each isomer, calculations were performed at the B3LYP-D3BJ/6-311++G(d,p) (blue curve) and MP2/6-311++G(d,p) (black curve) levels of theory.

B3LYP-D3BJ/6-311++G(d,p) levels of theory to obtain ground state rotational constants B_0^{ξ} and centrifugal distortion constants, as also given in Table 1.

2.2. Methyl Internal Rotation

The barrier height to internal rotation of the methyl group was also calculated at all levels used for geometry optimizations by optimizing the transition state where the H7 atom and the cyano group are in trans orientation (see Figure 1 for atom numbering and Figure 2 for molecular configurations). The torsional barrier is taken as the energy difference between the transition state and the corresponding minimum configurations. The results are summarized in Table S-2 in the Supplementary Materials.

At the MP2/6-311++G(d,p) and B3LYP-D3BJ/6-311++G(d,p) levels of theory, we calculated potential energy curves for both *Z* and *E* isomers, as depicted in Figure 2, to determine the V_3 and V_6 contributions. This was done by varying the dihedral angle $\alpha = \angle(C_1, C_2, C_3, H_7)$ in steps of 10° for a total of 120°, which was sufficient taking into account the C_{3v} symmetry of the methyl group. All other geometries parameters were optimized. Using a Fourier expansion to parameterize the energy points, we obtain V_3 potential values of 447.7 cm^{-1} (MP2) and 483.1 cm^{-1} (B3LYP-D3BJ) and the respective V_6 contributions of 21.4 cm^{-1} and 6.9 cm^{-1} for the *Z* isomer. The values of the E isomer are V_3/V_6 = 672.2/31.4 cm^{-1} (MP2) and 657.8/19.4 cm^{-1} (B3LYP-D3BJ).

2.3. ^{14}N nuclear quadrupole coupling constants

The NQCCs χ_{ij} can be used to model the splittings between the hyperfine components caused by the $I = 1$ spin of the ^{14}N nucleus. They are proportional to the electric field gradient (EFG) tensor components q_{ij} ($i, j = a, b, c$) at the quadrupole nucleus location:

$$\chi_{ij} = (eQ/h)\cdot q_{ij} \quad (1)$$

where e is the electronic charge, Q the electric quadrupole moment of the nitrogen nucleus, and h the Planck's constant. We applied Bailey's calibration[39] to calculate the NQCCs by calculating the ^{14}N EFG tensor at the B3PW91/6-311+G(d,p) level of theory recommended for molecules containing a π-conjugated system[40] on the geometry optimized at the MP2/6-311++G(d,p) level. This method has yielded very reliable ^{14}N NQCCs in many previous studies.[41-43] The obtained NQCC values are χ_{aa} = −1.7593 MHz, χ_{bb} = −0.0390 MHz, χ_{cc} = 1.7983 MHz, χ_{ab} = −2.9288 MHz for the *Z* isomer. They are χ_{aa} = −3.4687 MHz, χ_{bb} = 1.7172 MHz, χ_{cc} = 1.7515 MHz, χ_{ab} = −1.6240 MHz for the *E* isomer. By symmetry, χ_{ac} and χ_{bc} are zero.

3. Microwave spectroscopy

3.1. Spectral assignment

We started the spectral assignment with the more stable *Z* isomer, but the same procedure was applied for the *E* isomer afterwards. To access starting data, the five *a*-type and the five *b*-type transitions reported by Lesarri et al.[19] with resolved quadrupole hyperfine structure were remeasured and fitted with the *XIAM* program.[23] With prediction from this *XIAM* fit, more *a*- and *b*-type transitions were found and identified by their hyperfine structure. The three strongest hyperfine components were detected for almost all observed transitions, as shown exemplarily in Figure 3 for the $3_{03} \leftarrow 2_{02}$ rotational transition. Due to the torsional barrier height of ≈ 500 cm^{-1} of the methyl group, the separation of the A and E torsional components is in a range that both components are often visible in the detected frequency range of a high-resolution spectrum. The ^{14}N nuclear quadrupole hyperfine structure of both torsional components are identical within the experimental errors (see Figure 3). The spectrum is dominated by *a*-type transitions because the molecular dipole moment is mainly oriented along the inertial *a*-axis, and the *b*-type transitions are consequently weaker (see Table 1). Nevertheless, the number of detected *b*-type transitions was sufficient to determine the *A* rotational constant accurately. As the dipole moment component in the *c*-direction is zero, *c*-type transitions were not observable. The final fit of the *Z* isomer contains 330 lines with the fitted parameters shown in Table 2 and a root-mean-square (rms) deviation of 3.2 kHz. The spectrum of the *E* isomer is weaker (see an example of the $4_{14} \leftarrow 3_{13}$ transition shown in Figure 3, and the final fit of this isomer only includes 248 lines. The rms deviation of 3.3 kHz is also within the measurement accuracy. For comparison, the same datasets were fitted using the *BELGI-C_s-hyperfine* code[24] which also achieve satisfactory rms deviations for both isomers, although the parameters are not as well determined as in *XIAM* due to the high barrier and the low

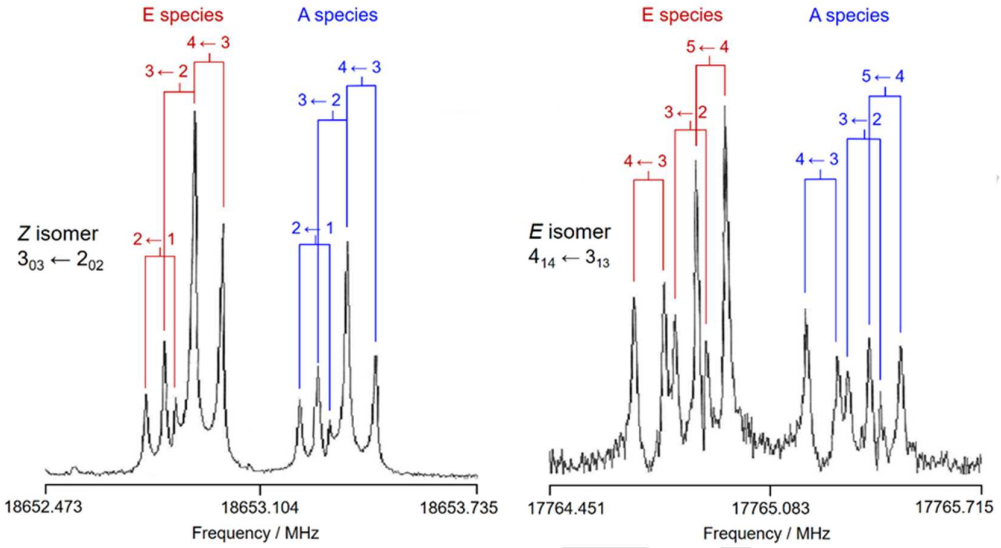

Figure 3. Two typical spectra of the *a*-type *R*-branch rotational transitions $3_{03} \leftarrow 2_{02}$ of the *Z* isomer and $4_{14} \leftarrow 3_{13}$ of the *E* isomer. The brackets indicate Doppler doublets. The A and E species are color-coded with the hyperfine components given as $F' \leftarrow F$. The intensities of the two spectra are normalized.

Table 2. Molecular parameters of both *Z* and *E* isomers of 1-cyanopropene in the principal axis system obtained by the program *XIAM* (this work) compared with the results from previous studies.

		***Z* isomer**		***E* isomer**		
Par.[a]	Unit	*XIAM*	Lessari et al.[19]	*XIAM*	Lessari et al.[19]	Hsu&Flygare[18]
A	MHz	11854.36730(50)	11854.449(10)[b]	38047.55(97)	38053.406(43)[b]	38054.0(4)[b]
B	MHz	3524.634723(95)	3524.6977(15)[b]	2297.27802(12)	2297.06890(72)[b]	2297.06(2)[b]
C	MHz	2759.718547(97)	2759.74293(73)[b]	2194.98555(11)	2195.18358(60)[b]	2195.21(2)[b]
Δ_J	kHz	2.7278(12)	2.73153(84)[b]	0.28550(90)	0.283422(46)[b]	
Δ_{JK}	kHz	−18.2631(84)	−18.2106(53)[b]	−17.325(17)	−17.3321(34)[b]	
Δ_K	MHz	0.0658(10)	0.065801(59)[b]	1.31(97)	0[b,c]	
δ_J	kHz	0.87398(36)	0.87471(54)[b]	0.03167(57)	0.029727(31)[b]	
δ_K	kHz	5.223(16)	5.253(17)[b]		−1.124(64)[b]	
I_α	uÅ^2	3.159[d]	3.106[d]	3.159[d]		3.23[d]
V_3	cm^{-1}	478.325(28)	485.180(70)	674.632(76)		664.5(70)
$D_{\pi^2 J}$	MHz	−0.2165(58)				
$D_{\pi^2 K}$	MHz	1.142(30)				
$\angle(i,a)$	°	76.136(13)	77.249[d]	13.118(30)		
$\angle(i,b)$	°	13.864(13)	12.75[d]	76.882(30)		
$\angle(i,c)$	°	90.0[e]	90.0[e]	90.0[e]		
χ_{aa}	MHz	−1.9054(15)	−1.8958(49)	−3.7150(24)	−3.7192(70)	−3.7(1)
χ_{bb}	MHz	−0.1024(17)	−0.1055(65)	1.7665(30)	1.7729(92)	1.70(5)
χ_{cc}	MHz	2.0078(36)	2.0013(65)	1.9485(67)	1.9463(92)	2.0(15)
rms[f]	kHz	3.2	34[b]	3.3	46[b]	
N_A/N_E[g]		167/163	111/0[b]	127/121	75/0[b]	

[a] All parameters refer to the principal axis system. Watson's A reduction and I^r representation were used. Standard errors are expressed in units of the last digits.

[b] Obtained from A species separate fits.

[c] Assumed value.

[d] Fixed value. The value calculated at the MP2/6-311++G(d,p) level is 3.168 uÅ^2.

[e] Fixed due to symmetry.

[f] Root-mean-square deviation of the fit.

[g] Number of rotational components of the torsional A and E symmetry species, including ^{14}N NQCC components for the XIAM fits and excluding ^{14}N NQCC components for the Lesarri et al. fits.

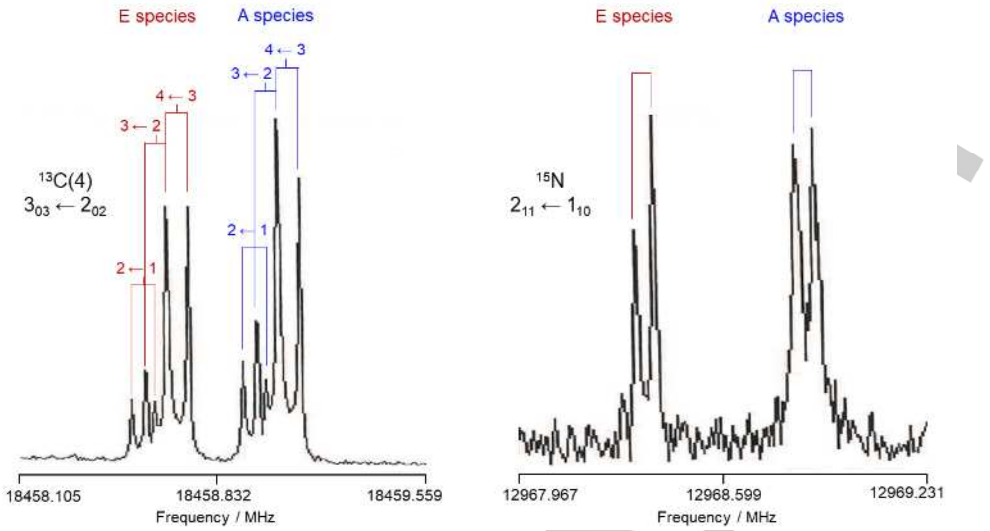

Figure 4. A typical spectrum of the $2_{11} \leftarrow 1_{10}$ transition of the ^{15}N isotopologue and of the $3_{03} \leftarrow 2_{02}$ transition of the ^{13}C(2) isotopologue. The intensities of the two spectra are normalized.

rotation-torsion coupling constant ρ in the case of *Z*-1-cyanopropene. The frequency list including fit residuals is available in Table S-3 in the Supplementary Materials. The *BELGI-Cs-hyperfine* parameters obtained in the rho-axis system are available in Table S-4.

3.2. Minor isotopologue spectra of the *Z* isomer

3.2.1. Spectral assignment and fits

Using isotopic shift calculations, it was straightforward to find the spectra of the four ^{13}C and the ^{15}N isotopologues of the more stable *Z* isomer. The line intensity of the ^{15}N spectrum with natural abundance of 0.35% was quite acceptable because of the ^{15}N nuclear spin I = ½ that does not cause quadrupole hyperfine splittings on the rotational transitions. Typical spectra of the $3_{03} \leftarrow 2_{02}$ transition of the ^{13}C(2) isotopologue and the $2_{11} \leftarrow 1_{10}$ transition of the ^{15}N isotopologue are illustrated in Figure 4. Providing from ab initio calculations that the influence of isotopic substitution on the centrifugal distortion constants is negligible (see Table S-5 in the Supplementary Materials), the values for minor isotopologue fits were fixed to those of the parent species fit given in Table 2, except for D_J and D_{JK} which are needed to achieve good rms deviations. The higher order parameters $D_{\pi^2 J}$ and $D_{\pi^2 K}$ for the methyl internal rotation were also fixed to the values of the parent species. Molecular parameters of all *Z*-1-cyanopropene minor isotopologue fits are summarized in Table 3. The frequency lists are in Table S-6 of the Supplementary Materials.

3.2.2 Structure determination

From the six sets of rotational constants (the parent species, four ^{13}C isotopologues, and the ^{15}N isotopologue), we could determine the heavy atom substitution structure r_s using Kraitchman's equations[44] as implemented in the programs *KRA* and *EVAL*.[45] The signs of the atom coordinates were taken from the optimized geometry given in Table S-1 in the Supplementary Materials and Costain's rule was used to calculate the uncertainties.[46] The atom coordinates determined by *KRA* are given in Table 4; the bond lengths and bond angles from *EVAL* are in Table 5.

The substitution structure r_s is a traditional and simple method to determine molecular geometry parameters, especially in earlier microwave studies, where quantum chemistry techniques had not yet been developed. The B_0^ξ experimental rotational constants are directly utilized, and bond lengths and bond angles are therefore from the vibrational ground state. With continuously increasing computational resources, quantum chemistry has become a powerful tool to support microwave spectroscopy. However, equilibrium structures r_e obtained from geometry optimizations cannot be directly compared with the r_s structure since they refer to different states. A simple alternative is to correct the experimental B_0^ξ rotational constants of all observed isotopologues with the difference $\Delta B = B_{0,\text{calc.}}^\xi - B_{e,\text{calc.}}^\xi$ obtained from cubic force field calculations before inputting them in the program *KRA* and *EVAL* to access the so-called semi-experimental equilibrium structure r_e^{SE} that can be compared to the r_e structure. This has been the method of choice for many theoretical groups and generally accepted in many experimental microwave labs.[47-51] The atom coordinates of the r_e^{SE} structure with ΔB calculated at the MP2/6-311++G(d,p) level are collected in Table 4. The bond angles and bond lengths are given in Table 5 and illustrated in Figure 5. For comparison, values from the equilibrium structure are also shown in Tables 4 and 5.

4. Discussion

Rotational transitions due to the *E* and the *Z* isomers of 1-cyanopropene were identified and assigned in the microwave spectrum recorded under jet-cooled conditions, including those of all ^{13}C and the ^{15}N isotopologues of the more stable Z isomer. The overall fits obtained with the *XIAM* program comprising 330 and 248 lines reach rms deviations of 3.2 kHz and 3.3 kHz, respectively, which are within the estimated accuracy of the

Table 3. Molecular parameters all ^{13}C isotopologues and the ^{15}N isotopologue fits of the *Z*-1-cyanopropene obtained from the program *XIAM*. Atoms are numbered according to Figure 1.

Par.[a]	Unit	^{13}C(1)	^{13}C(2)	^{13}C(3)	^{13}C(4)	^{15}N
A_0	MHz	11849.62885(84)	11590.5052(14)	11629.0635(11)	11783.0044(12)	11770.9483(22)
B_0	MHz	3494.02452(36)	3524.82863(61)	3459.45642(49)	3485.88290(49)	3424.95713(93)
C_0	MHz	2740.66529(31)	2745.22650(53)	2707.51709(35)	2732.07932(42)	2693.84131(82)
Δ_J	kHz	2.641(13)	2.747(22)	2.700(14)	2.554(18)	2.514(35)
Δ_{JK}	kHz	–18.104(43)	–17.899(73)	–18.293(59)	–17.192(96)	–17.79(11)
V_3	cm^{-1}	478.30(14)	477.92(24)	479.40(17)	478.85(21)	478.59(40)
∠(*i*,*a*)	°	76.083(25)	77.211(43)	76.389(32)	76.437(53)	76.821(67)
∠(*i*,*b*)[b]	°	13.917(25)	12.789(43)	13.611(32)	13.563(53)	13.179(67)
χ_{aa}	MHz	–1.8966(33)	–1.9051(42)	–1.8079(34)	–1.9450(38)	
χ_{bb}	MHz	–0.1104(43)	–0.1033(69)	–0.2032(56)	–0.0663(58)	
χ_{cc}	MHz	2.0070(95)	2.008(16)	2.011(13)	2.011(14)	
N[c]		55	56	60	51	19
rms[d]	kHz	2.5	4.2	3.5	3.4	3.2

[a] All parameters refer to the principal axis system. The centrifugal distortion constants except Δ_J and Δ_{JK} are fixed to values determined for the parent species given in Table 2 for all ^{13}C and ^{15}N isotopologues.

[b] ∠(*i*,*c*) is fixed to 90° in all fits due to symmetry.

[c] Number of lines.

[d] Root-mean-square deviation of the fit.

Table 4. Substitution r_s and semi-experimental equilibrium r_e^{SE} atom positions of the more stable *Z* isomer of 1-cyanopropene obtained from isotopic substitutions with Kraitchman's equations[44] as implemented in the program *KRA*.[45] For comparison, the equilibrium atom positions from the r_e geometry optimized at the MP2/6-311++G(d,p) level of theory are also given.

	r_s		r_e^{SE}		r_e		
	a / Å	*b* / Å	*a* / Å	*b* / Å	*a* / Å	*b* / Å	*c* / Å
C(1)	0.077(20)	–0.9919(15)	0.047(32)	–0.9895(15)	0.01523	–0.99394	0.0
C(2)	1.2683(12)	–0.5153(29)	1.2682(12)	–0.5113(29)	1.27615	–0.51623	0.0
C(3)	1.64679(91)	0.9272(16)	1.64281(91)	0.9266(16)	1.65760	0.93066	0.0
C(4)	–1.1271(13)	–0.132(11)	–1.1218(13)	–0.146(10)	–1.13062	–0.13278	0.0
N(10)	–2.05515(73)	0.5666(27)	–2.05271(73)	0.5652(27)	–2.07732	0.56785	0.0

Table 5. Bond lengths, bond angles, and dihedral angles deduced from the substitution r_s and semi-experimental equilibrium r_e^{SE} structure of the more stable *Z* isomer of 1-cyanopropene obtained using the program *EVAL*.[45]

	r_s	r_e^{SE}	r_e
Bonds lengths / Å			
C1–C4	1.479(17)	1.441(27)	1.43338
C1–C2	1.283(18)	1.312(30)	1.34838
C2–C3	1.4913(32)	1.4858(33)	1.49632
C4–N10	1.1615(71)	1.1715(66)	1.17776
Bond angles / °			
C1–C2–C3	126.50(37)	125.99(54)	125.519
C4–C1–C2	122.66(41)	122.79(44)	122.323

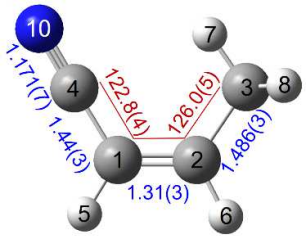

Figure 5. Bond lengths (blue, in Å), bond angles (dark red, in degrees) of the semi-experimental equilibrium structure r_e^{SE} of the *Z* isomer of 1-cyanopropene.

measurements. Fitted molecular parameters are the rotational constants, quartic centrifugal distortion constants, the angle between the principal *a*-axis and the methyl rotor axis, the V_3 term of the potential, the NQCCs, as well as two higher order parameters for the internal rotation $D_{\pi^2 J}$ and $D_{\pi^2 K}$ in the case of the *Z* isomer. Since only torsional ground state transitions are present in the jet-cooled spectrum, for both isomers, the rotational constant F_0 of the methyl group was fixed at 160 GHz, a value often found for methyl groups, to avoid the correlation with V_3. This corresponds to a moment of inertia I_α of 3.159 uÅ^2. The accuracy of the *XIAM* fits were confirmed by using the program *BELGI* to refit the same data sets.

The equilibrium rotational constants calculated using different combinations of methods and basis sets mentioned in section 2.1. have shown that all tested levels with the B3LYP, PBE0, and ωB97X-D methods are not suitable for both *E* and *Z* isomers. The M06 levels with the modest 6-31 basis set performs well for both isomers, independently whether diffuse functions are included or not. Staying with the same method M06, Dunning's cc-pVDZ without diffuse function works well for the *Z* isomer, but in contrast, the aug function is required for the *E* isomer. Exactly the same basis sets perform well while combined with the MN15 method. In this case, both cc-pVDZ and aug-cc-pVDZ work. This is not surprising if considering that both methods have been developed by Truhlar *et al*. Turning to the *ab initio* MP2 method, globally, the agreement between calculated and experimental values is better. For the *Z* isomer, the 6-311++G(d,p) basis set combined with (2d,2p) and (ndf,npd) (n = 1, 2, 3) polarisation functions and the (aug)-cc-pVTZ basis sets are most suitable. For the *E* isomer, only the 6-311++G(df,pd) basis set among those mentioned above works well. Interestingly, the MP2/6-31G(d,p) level that has been recommended for many molecules containing an aromatic ring also gives results that are in very good agreement with the experimental values. Benchmarking of other propene derivatives is needed to refine this finding. Furthermore, not only the rotational constants, but also the methyl internal rotation barrier is benchmarked, as presented in Table S-2 in the Supplementary Materials. Not like for the rotational constants where large fluctuation was found while using different levels of theory, most of the levels yield well predicted values for the torsional barrier.

Compared to previous work by Lesarri et al.,[19] the rotational constants determined from the present fits are in good agreement but better determined for the *Z* isomer, and differ significantly for the *E* isomer. The reason is that our rotational constants are deduced from global fits considering both the A and the E torsional states, while previous rotational constants are from separately fitting of only the A sub-state. Regarding the purpose of structure determination, the rotational constants in use should be physically meaningful and therefore should be taken from global fitting. Values of centrifugal distortion constants and NQCCs of the present work and Ref. [19] are essentially the same. Concerning the V_3 potential value, our value of 478.325(28) cm^{-1} and literature value of 485.180(70) cm^{-1} [19] for the Z isomer as well as 674.632(76) cm^{-1} and 664.5(70) cm^{-1} [18] for the E isomer are very different. This is mainly because the I_α parameter is fixed to different values due to correlation with V_3.

Several microwave spectroscopic investigations are available for 1-substituted propene derivatives, and the experimental torsional barriers hindering the methyl internal rotation are summarized in Figure 6. For all six molecules in Figure 6, the *Z* isomer is more stable than the *E* isomer. Theoretical investigations[52] have shown that the higher stability of the *Z* isomer is mainly due to the attractive intramolecular non-bonded electrostatic interaction between the positively charged in-plane hydrogen atom of the methyl group and the substituent, as confirmed by the charge distribution from NBO calculations[53] shown in Figure 6. This is a rare finding[54] because electrostatic interaction is only possible if the distance between the two interacting partners is shorter than the sum of the van der Waals radii, which is the case of all molecules illustrated in Figure 6.[55] Therefore, the *Z* form features a special characteristic that the equilibrium structure has one hydrogen atom of the methyl group eclipsed to the substitution at the 1-position, while the staggered configuration is the transition state (see also Figure 2).

The higher stability of the *Z* isomer with the eclipsed configuration being the equilibrium structure brings several consequences. First of all is the opening up of the C(1)-C(2)-C(3) angle to 126.0(5)° due to the nearness of the methyl and the cyano groups. As can be recognized from Figure 5 and Table 5, this angle is approximately 3.2° larger than the C(4)-C(1)-C(2) angle of 122.8(4)° in 1-cyanopropene. Other geometry parameters such as bond lengths reflect well the single, double, and triple bond characters.

Secondly, we can clearly recognize that the barrier is radically lower in the *Z* configuration of all six molecules in Figure 6. To explain phenomena concerning the methyl torsional barrier values, steric and electrostatic effects often come into play. If considering the steric hindrance, then the barrier value of the *Z* isomer must be greater than that of the *E* isomer, but the observation is the opposite, which is known as the 1-propene "*cis* effect". The non-bonded repulsive interaction between the methyl group and the 1-substituent repels the H(7) atom from the substituent, thereby lowering the methyl torsional barrier. The variation in the barrier values among molecules (**1**-**6**) should arise from a combination of electrostatic attraction strength represented mainly by the charges, the non-bonded distances, and the van der Waals radius. We note that different sources yield different values for the charges, and the values used here are those from NBO calculations. Electrostatic information could be transferred also through the π-delocalization, reflected by the variation of the methyl barrier found for the *E* isomers, especially between the groups of molecules (**1**-**3**) and (**4**-**6**) in Figure 6. However, lacking direct interactions of both electrostatic attraction and steric repulsion, the changes are not as radical as in the case of the *Z* isomers.

Conclusions

The microwave spectra of the *Z* and the *E* isomers of 1-cyanopropene were recorded in the frequency range between 2.0 and 40.0 GHz, revealing splittings consisting of A-E doublets due to internal rotation of the methyl group and hyperfine structures due to the ^{14}N nuclear quadrupole coupling effect for both isomers. Spectra of all ^{13}C and ^{14}N minor isotopologues of the more stable *Z* isomer were detected, and the heavy atom microwave structure could be determined. The higher stability of the *Z* isomer due to non-bonded intramolecular electrostatic attraction between the methyl group and the 1-substituent causes a slight opening of about 3.2° of the C(1)-C(2)-C(3) and a radical decrease of the methyl torsional barrier due to consequent steric repulsion.

Experimental Section

A commercial sample of 1-cyanopropene containing a mixture of both isomers (*E*- and *Z*-1-cyanopropene) was purchased and used without further purification. The microwave spectra of 1-cyanopropene were recorded between 2.0 and 40.0 GHz using two molecular jet FTMW spectrometers, producing the molecular

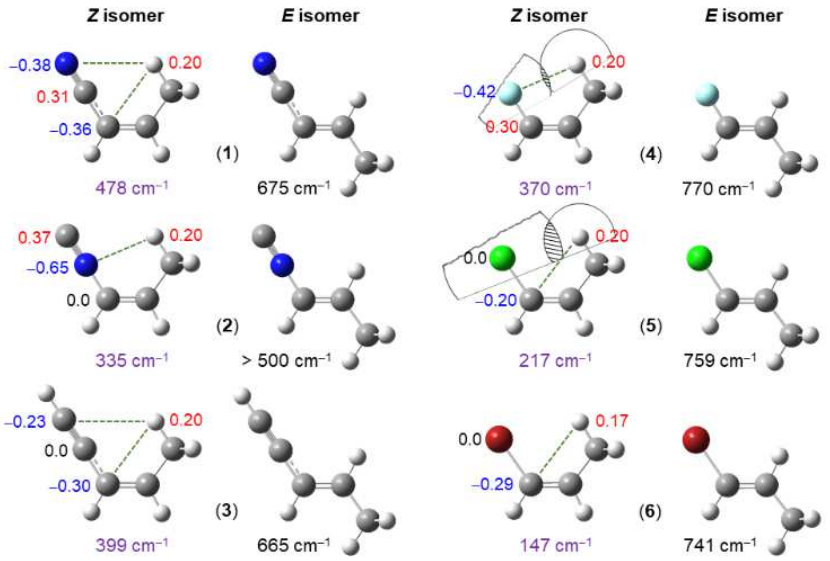

Figure 6. Comparison of the experimental barriers to methyl internal rotation (given in lila for the *Z* isomers and black for the *E* isomers) in 1-substituted propene derivatives. (**1**) 1-cyanopropene (this work), (**2**) 1-isocyanopropene,[56] (**3**) 3-pentene-1-yne,[57],[58] (**4**) 1-fluoropropene,[59],[60] (**5**) 1-chloropropene,[61],[62] and (**6**) 1-bromopropene.[63] The blue and red values at the *Z* isomers indicate the partial charges obtained from NBO calculations. Possible non-bonded electrostatic interactions are presented as dotted green lines. Van der Waals radii are shown exemplarily for molecules (4) and (5).

beam by adiabatic expansion of a mixture of 0.5% 1-cyanopropene in argon at a stagnation pressure of about 1.5 bar.[20],[21] As the rotational temperature in the molecular jet amounts only a few K, rotational transitions up to $J = 8$ could be measured. Due to the low vibrational temperature, no vibrationally excited states ($v > 0$) were observed. All lines split into two Doppler components due to the co-axial arrangement between the molecular beam and the resonators. The instrumental resolution is 2 kHz,[64] but the estimated measurement accuracy is about 4 kHz, corresponding to 1/10 of the averaged full-width at half-maximum (FWHM).

Acknowledgements

T. A. Nguyen thanks the Université Paris Cité for a PhD fellowship and the HRMS committee of the 28th Conference on High Resolution Molecular Spectroscopy, Dijon, France, for the opportunity to present the results of this work as an oral contribution. The work was supported by the Agence Nationale de la Recherche ANR (Project ID ANR-18-CE29-0011) and the European Union (ERC, 101040480-LACRIDO), and partly by the French National program LEFE (Les Enveloppes Fluids et l'Envi ronnement).

Keywords: rotational spectroscopy • microwave spectroscopy • methyl internal rotation • ab initio calculations • 1-cyanopropene

References

[1] M. Berglund, M. E. Wieser, Pure Appl. Chem. **2011**, *83*, 397–410.
[2] W. Gordy and R. L. Cook, *Microwave molecular spectra*, Vol. 18, *3rd Ed.*, Wiley, New York, **1984**.
[3] B. Tercero, I. Kleiner, J. Cernicharo, H. V. L. Nguyen, A. López, G. M. Muñoz Caro, *Astrophys. J. Lett.* **2013**, *770*, 13.
[4] A. McKellar, *Publ. Astron. Soc. Pac.* **1940,** *52*, 187-192.
[5] C. P. Endres, S. Schlemmer, P. Schilke, J. Stutzki, H. S. P. Müller, *J. Mol. Spectrosc.* **2016**, *327*, 95-104.
[6] B. A. McGuire, Astrophys. *J. Suppl. Ser.* **2022**, *259*, 30.
[7] S. M. Fortman, J. P. McMillan, C. F. Neese, S. K. Randall, A. J. Remijan, T. L. Wilson, F. C. De Lucia, *J. Mol. Spectrosc.* **2012**, *280*, 11-20.
[8] B. A. McGuire., A. M. Burkhardt, S. Kalenskii, C. N. Shingledecker, A. J. Remijan, E. Herbst, M. C. McCarthy, *Science* **2018**, *359*, 202.
[9] B. A. McGuire, A. M. Burkhardt, R. A. Loomis, K. L. K Lee, S. B. Charnley, M. A. Cordiner, E. Herbst, S. Kalenskii, E. Momjian, E. R. Willis, C. Xue, A. J. Remijan, M. C. McCarthy, *Astrophys. J. Lett.* **2020**, *900*, 10.
[10] K. L. K. Lee, P. B. Changala, R. A. Loomis, A. M. Burkhardt, C. Xue, M. A. Cordiner, S. B. Charnley, M. C. McCarthy, B. A. McGuire, *Astrophys. J. Lett.* **2021**, *910*, 2.
[11] K. L. K. Lee, R. A. Loomis, A. M. Burkhardt, I. R. Cooke, C. Xue, M. A. Siebert, C. N. Shingledecker, A. J. Remijan, S. B. Charnley, M. C. McCarthy, B. A. McGuire, *Astrophys. J. Lett.* **2021**, *908*, 11.
[12] C. N. Shingledecker, K. L. K. Lee, J. T. Wandishin, N. Balucani, A. M. Burkhardt, S. B. Charnley, R. A. Loomis, M. Schreffler, M. A. Siebert, M. C. McCarthy, B. A. McGuire, *A&A* **2021**, *652*, 12.
[13] B. A. McGuire, R. A. Loomis, A. M. Burkhardt, K. L. K. Lee, C. N. Shingledecker, S. B. Charnley, I. R. Cooke, M. A. Cordiner, E. Herbst, S. Kalenskii, M. A. Siebert, E. R. Willis, C. Xue, A. J. Remijan, M. C. Mccarthy, *Science* **2021**, *371*, 1265-1269.
[14] C. Cabezas, J. Tang, M. Agúndez, K. Seiki, Y. Sumiyoshi, Y. Ohshima, B. Tercero, N. Marcelino, R. Fuentetaja, P. de Vicente, Y. Endo, J. Cernicharo, *A&A* **2023**, *676*, 5.
[15] J. Cernicharo, R. Fuentetaja, C. Cabezas, M. Agúndez, N. Marcelino, B. Tercero, J. R. Pardo, P. De Vicente, *A&A* **2022**, *663*, 5.
[16] R. A. Beaudet, *J. Chem. Phys.* **1963**, *38*, 2548-2552.

[17] M. Suzuki, K. Kozima, *J. Mol. Spectrosc.* **1970**, *33*, 407-413.
[18] S. L. Hsu, W. L. Flygare, *J. Mol. Spectrosc.* **1971**, *37*, 92-99.
[19] A. G. Lesarri, J. Cosléou, X. Li, G. Wlodarczak, J. Demaison, *J. Mol. Spectrosc.* **1995**, *172*, 520-535.
[20] J.-U. Grabow, W. Stahl, H. Dreizler, *Rev. Sci. Instrum.* **1996**, *67*, 4072-4084.
[21] I. Merke, W. Stahl, H. Dreizler, *Z. Naturforsch. A: Phys. Sci.* **1994**, *49a*, 490-496.
[22] R. C. Woods, *J. Mol. Spectrosc.* **1966**, *21*, 4-24.
[23] H. Hartwig, H. Dreizler, *Z. Naturforsch.* **1996**, *51a*, 923-932.
[24] R. Kannengießer, W. Stahl, H. V. L. Nguyen, I. Kleiner, *J. Phys. Chem. A* **2016**, *120*, 3992-3997.
[25] M. J. Frisch, G. W. Trucks, H. B. Schlegel, G. E. Scuseria, M. A. Robb, J. R. Cheeseman, G. Scalmani, V. Barone, G. A. Petersson, H. Nakatsuji, X. Li, M. Caricato, A. V. Marenich, J. Bloino, B. G. Janesko, R. Gomperts, B. Mennucci, H. P. Hratchian, J. V. Ortiz, A. F. Izmaylov, J. L. Sonnenberg, D. Williams-Young, F. Ding, F. Lipparini, F. Egidi, J. Goings, B. Peng, A. Petrone, T. Henderson, D. Ranasinghe, V. G. Zakrzewski, J. Gao, N. Rega, G. Zheng, W. Liang, M. Hada, M. Ehara, K. Toyota, R. Fukuda, J. Hasegawa, M. Ishida, T. Nakajima, Y. Honda, O. Kitao, H. Nakai, T. Vreven, K. Throssell, J. A. Montgomery, Jr., J. E. Peralta, F. Ogliaro, M. J. Bearpark, J. J. Heyd, E. N. Brothers, K. N. Kudin, V. N. Staroverov, T. A. Keith, R. Kobayashi, J. Normand, K. Raghavachari, A. P. Rendell, J. C. Burant, S. S. Iyengar, J. Tomasi, M. Cossi, J. M. Millam, M. Klene, C. Adamo, R. Cammi, J. W. Ochterski, R. L. Martin, K. Morokuma, O. Farkas, J. B. Foresman and D. J. Fox, *Gaussian 16*, *Revision B.01*, Gaussian, Inc., Wallingford CT, **2016**.
[26] A. D. Becke, *J. Chem. Phys.* **1993**, *98*, 5648-5652.
[27] C. Lee, W. Yang, R. G. Parr, *Phys. Rev. B* **1988**, *37*, 785-789.
[28] S. Grimme, J. Antony, S. Ehrlich, H. Krieg, *J. Chem. Phys.* **2010**, *132*, 154104.
[29] S. Grimme, S. Ehrlich, L. Goerigk, *J. Comput. Chem.* **2011**, *32*, 1456-1465.
[30] T. Yanai, D. P. Tew, N. C. Handy, *Chem. Phys. Lett.* **2004**, *393*, 51-57.
[31] J. D. Chai, M. Head-Gordon, *Phys. Chem. Chem. Phys.* **2008**, *10*, 6615-6620.
[32] C. Adamo, V. Barone, *J. Chem. Phys.* **1999**, *110*, 6158-6170.
[33] H. S. Yu, X. He, S. L. Li, D. G. Truhlar, *Chem. Sci.* **2016**, *7*, 5032-5051.
[34] Y. Zhao, D. G. Truhlar, *Theor. Chem. Acc.* **2018**, *120*, 215-241.
[35] C. Møller, M. S. Plesset, *Phys. Rev.* **1934**, *46*, 618-622.
[36] R. J. Bartlett, M. Musiał, *Rev. Mod. Phys.* **2007**, *79*, 291-352.
[37] T. H. Dunning, *J. Chem. Phys.* **1989**, *90*, 1007-1023.
[38] M. J. Frisch, J. A. Pople, J. S. Binkley, *J. Chem. Phys.* **1984**, *80*, 3265-3269.
[39] W. C. Bailey, *Chem. Phys.* **2000**, *252*, 57-66.
[40] R. Kannengießer, W. Stahl, H. V. L. Nguyen, W. C. Bailey, *J. Mol. Spectrosc.* **2015**, *317*, 50-53.
[41] Q. T. Tran, A. Errouane, S. Condon, C. Barreteau, H. V. L. Nguyen, C. Pichon, *J. Mol. Spectrosc.* **2022**, *388*, 111685.
[42] S. Baweja, E. Antonelli, S. Hussain, A. Fernández-Ramos, I. Kleiner, H. V. L. Nguyen, M.E. Sanz, *Molecules* **2023**, *28*, 2153.
[43] H. E. Hadki, K. J. Koziol, O. K. Kabbaj, N. Komiha, I. Kleiner, H. V. L. Nguyen, *Molecules* **2023**, *28*, 3419.
[44] J. Kraitchman, *Am. J. Phys.* **1953**, *21*, 17-24.
[45] Z. Kisiel, PROSPE-Programs for ROtational SPEctroscopy, see http://info.ifpan.edu.pl/~kisiel/prospe.htm.
[46] C. C. Costain, *Am. Crystallogr. Assoc.* **1966**, *2*, 157-164.
[47] B. J. Esselman, B. K. Amberger, J. D. Shutter, M. A. Daane, J. F. Stanton,R. C. Woods, R. J. McMahon, *J. Chem. Phys.* **2013**, *139*, 224304.
[48] J. Demaison, A. G. Császár, L. D. Margulès, H. D. Rudolph, *J. Phys. Chem. A* **2011**, *115*, 14078-14091.
[49] S. Herbers, P. Kraus, J.-U. Grabow, *J. Chem. Phys.* **2019**, *150*, 144308.
[50] F. Xie, M. Fusè, A. S. Hazrah, W. Jäger, V. Barone, Y. Xu, *Angew. Chem. Int.* **2020**, *59*, 22427-22430.
[51] H. V. L. Nguyen, J.-U. Grabow, *ChemPhysChem* **2020**, *21*, 1243-1248.
[52] K. B. Wiberg, Y. Wang, G. A. Petersson, W.F. Bailey, *J. Chem. Theory Comput.* **2009**, *5*, 1033-1037.
[53] E. D. Glendening, C. R. Landis, F. Weinhold, *WIREs Comput. Mol. Sci.* **2012**, *2*, 1-42.
[54] T. Uchimaru, J. Mizukado, *J. Fluorine Chem.* **2021**, *245*, 109772.
[55] A. Bondi, *J. Phys. Chem.* **1964**, *68*, 441-451.
[56] S. Samdal, H. Møllendal, J. C. Guillemin, *J. Phys. Chem. A* **2012**, *116*, 8833-8839.
[57] R. G. Ford, R. A. Beaudet, *J. Chem. Phys.* **1971**, *55*, 3110-3113.
[58] R. G. Ford, L. B. Szalanski, *J. Mol. Spectrosc.* **1972**, *42*, 344-349.
[59] R. A. Beaudet, E. B. Wilson, *J. Chem. Phys.* **1962**, *37*, 1133-1138.
[60] S. Siegel, *J. Chem. Phys.* **1957**, *27*, 989-990.
[61] R. A. Beaudet, *J. Chem. Phys.* **1964**, *40*, 2705-2715.
[62] R. A. Beaudet, *J. Chem. Phys.* **1962**, *37*, 2398-2402.
[63] R. A. Beaudet, *J. Chem. Phys.* **1969**, *50*, 2002-2011.
[64] J.-U. Grabow, W. Stahl, *Z. Naturforsch.* **1990**, *45a*, 1043-1044.

Entry for the Table of Contents

FULL PAPER	
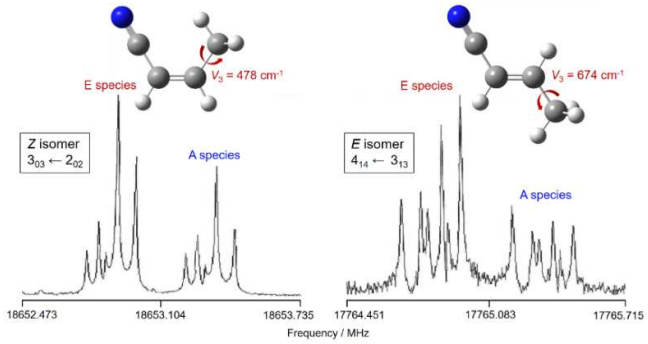	*Truong Anh Nguyen, Isabelle Kleiner, Martin Schwell, Ha Vinh Lam Nguyen** ***Page No. – Page No.*** **The heavy atom structure, "*cis* effect" on methyl internal rotation, and ^{14}N nuclear quadrupole coupling of 1-cyanopropene from quantum chemical and microwave spectroscopic analysis**

The gas-phase structures of 1-cyanopropene was determined by the interplay of quantum chemistry and microwave spectroscopy, revealing two isomers, *E* and *Z*. The higher stability of the *Z* isomer due to non-bonded intramolecular electrostatic attraction between the methyl group and the 1-substituent causes a slight opening of about 3.2° of the C(1)-C(2)-C(3) angle and a significant decrease of the methyl torsional barrier due to consequent steric repulsion.